ELSEVIER

Journal of Chromatography A, 750 (1996) 287–301

JOURNAL OF CHROMATOGRAPHY A

Hyphenated techniques for characterizing coal wastewaters and associated sediments

J. Pörschmann*, F.-D. Kopinke, M. Remmler, K. Mackenzie, W. Geyer, S. Mothes

Centre for Environmental Research Leipzig-Halle Ltd., Permoserstr. 15, 04318 Leipzig, Germany

Abstract

Capillary gas chromatography (cGC)–mass spectrometry (MS) and cGC–atomic emission detection (AED) were used for the analysis of extracts from highly contaminated wastewaters and associated sediments. The main extractable constituents in both the lignite wastewater and the sediments include phenols, PAHs, indenols and heterocyclic compounds. Pyrolysis (Py)–GC–MS and Py–GC–AED were used for characterizing the building blocks of the dissolved polymeric organic matter. Polymers of natural and anthropogenic origins could be clearly distinguished. The Py–MS studies performed with humic organic matter at both atmospheric pressure and high vacuum (in-source mode) indicate a high portion of pyrolysis residue (about 40%, w/w) upon heating to 700°C, irrespective of the pressure level. The products released include many low molecular weight compounds which are of limited value for characterizing the polymeric network.

Keywords: Coal; Water analysis; Sediments; Environmental analysis; Humic acids; Fulvic acids; Organic pollutants

1. Introduction

Wastewaters from pyrolytic lignite decomposition are known to be highly contaminated with organic pollutants covering a wide range of volatility and polarity. The coal wastewater investigated in the present study originates from a pond near Leipzig, having a volume of 2×10^6 m^3 and a surface area of 90 000 m^2. This wastewater pond has been left in its original state for three decades without any attempt at remediation. From this point of view it is an unique system, where a variety of organic compounds have had the opportunity to interact with each other in a concentrated aqueous solution under natural conditions [1]. The dark brown colour of the wastewater is attributed to the formation of dissolved, humin-like organic matter (HOM) having a concentration of about 300 mg C l^{-1}. Owing to their origin, their structure and their capability to enter into interactions with organic and inorganic pesticides, we call these polymers anthropogenic HOM [2]. Generally, the dissolved HOM is classified operationally into humic and fulvic acids.

Beyond basic scientific interest in the structure and properties of anthropogenic HOM, our interest is focused on remediating these highly contaminated sites. Therefore it is necessary to obtain knowledge of the quantity and quality of the organic pollutants as a prerequisite for developing remediation measures.

A severe difficulty when analyzing organic pollutants in both the coal wastewater and the sediment lies in their complexity. Therefore, the utilization of hyphenated techniques, which combine separation with identification, is preferred. For non-volatile samples a pretreatment step is advisable, generating volatile fragments which should reflect as far as

*Corresponding author.

0021-9673/96/$15.00
PII S0021-9673(96)00403-7

possible the original sample. The structure and the features of anthropogenic HOM are relatively unknown, in contrast to natural HOM which has been the subject of considerable interest for some decades (see [3–5] and literature cited therein).

The aim of this contribution is twofold, consisting of a pollutant identification and a matrix analysis part. The first part deals with the analysis of the highly contaminated wastewaters and sediments by means of hyphenated techniques including cGC–MS and cGC–AED. Liquid–liquid extraction and SFE were used to obtain organic extracts from the coal wastewater and the associated sediment, respectively. The second part describes the structural characterization of the anthropogenic HOM both dissolved in the wastewater and precipitated in the sediment. For this purpose, hyphenated techniques including Py–cGC–MS, TG–MS and TG–FTIR were utilized.

2. Experimental

2.1. Liquid–liquid extraction of the coal wastewater

50 ml wastewater (1:1 diluted with distilled water) was extracted twice with 50 ml benzene by vigorous shaking for 10 min. The extracts were then combined. The high amount of benzene is required to minimize the formation of emulsions due to surface activity of the HOM in the wastewater [6]. Deuterated standards (from Promochem Wesel, Germany, 10 ppm each for phenol, *o*-cresol, 3,4-dimethylphenol; 10 ppb each for PAHs naphthalene to benzo-[*a*]-pyrene; 1 ppm each for *n*-hexadecane, benzofurane, chinoline; all perdeuterated) were added to the benzene before extracting. The extract was dried with Na_2SO_4 and concentrated to 0.5 ml by evaporation in a rotary evaporator at 40 °C.

2.2. Isolation of humic and fulvic acids from coal wastewater and sediment

The isolation procedure consisting mainly of XAD- and ion-exchange column chromatography is detailed in [7,8].

2.3. Supercritical fluid extraction of the wastewater sediment

200 mg of the sediment to be extracted and the inert Hydromatrix material (to minimize cell dead volume effects) were filled to capacity into a 0.5 ml cartridge (ISCO, Lincoln, NE). The extraction was performed using an SFE 260D-ISCO device with a thermoadjustable restrictor. We utilized a two-step extraction procedure: first using pure carbon dioxide at 90 °C and 380 atm (1 atm=101 325 Pa) for 3 min static extraction and 10 min dynamic extraction, then adding 8% methanol polar modifier raising the temperature to 140 °C and the pressure to 490 atm (density 0.72 g ml^{-1}) for another 10 min, both at a constant flow-rate of 0.85 ml min^{-1}. For reasons of quantitative calibrations we preferred adding the deuterated standards onto the top of the cell before the extraction rather than spiking the trapping solvent with chloroform. The crude extract was concentrated as described above.

2.4. cGC–MS and cGC–AED

The following type of capillary and temperature program were used: 30 m×0.25 mm I.D. coated with 0.25 μm HP-5 (Hewlett-Packard, Palo Alto, CA, USA); from 45 °C (2 min isothermal) to 290 °C (8 min isothermal) at a ramp of 8 K min^{-1}. The capillaries were run in the constant flow mode (0.8 ml min^{-1}). 0.5 μl of the pre-concentrated extract solutions was injected splitless with a purge time of 1 min at an injector temperature of 270 °C. As cGC–MS device a Hewlett-Packard GC 5890 Series II coupled to a MSD 5971 (70 eV EI, m/z=33–320 u, scan rate 1.5 Hz) was used. As cGC–AED device the HP GC 5890 was coupled to a HP 5921A. The wavelengths (nm) monitored were as follows: 193.0 and 495.7 for carbon, 180.7 for sulphur, 174.2 for nitrogen, 178.1 for phosphorus, 777.2 for oxygen, 478.6 for bromine, 497.5 for chlorine.

2.5. Py–cGC–MS, Py–cGC–AED, Py(Methylation)–cGC–MS

For the analysis of non-volatile samples a pyrolysis step was performed prior to cGC–MS and cGC–AED. Samples of sediments and isolated

humic or fulvic acids (about 5–10 mg) were placed into a small quartz tube and heated using a flash pyrolyzer Pyroprobe 1000 (CDS, Oxford, USA). The pyrolysis parameters were as follows: 350 °C and 700 °C set temperature for thermodesorption and pyrolysis, respectively; interface temperature 250 °C; platinum coil heating rate 0.5 K ms^{-1}; isothermal period 10 s. The released compounds were flushed into the GC using the split injection at a split ratio of 1:25. The capillary column was a 50 m×0.32 mm column with a film thickness of 1.0 μm HP-5.

For pyrolysis-methylation experiments the sample (5 mg) was heated with tetramethylammonium hydroxide (50 μl 25%, w/w, TMAH in methanol) under reflux for some h. The solvent was then evaporated and the remaining syrup was transferred into the quartz tube of the pyrolyzer. The pyrolysis was performed in two steps: at 500 °C and at 800 °C for 10 s each.

2.6. TG–MS, TG–FTIR, Py–MS

The combined thermoanalytical apparatus used in our studies is depicted schematically in Fig. 1 and detailed below.

It consists of a thermobalance (TGA 50 from Shimadzu, Duisburg, Germany), a tube furnace (from Raytest, Straubenhardt, Germany), a gas chromatograph (GC 14A from Shimadzu), a quadrupole mass spectrometer (QMS) (QP 1100EX from Shimadzu, m/z=10–1000 u, EI and CI ionization mode) and two flash pyrolyzers (Pyroprobe 1000 and 2000 from CDS). The sample to be investigated can be treated in four reactors:

1. the thermobalance (1–100 mg sample, 30–900 °C, $dT/dt \leq 50$ K min^{-1}, p=0.1 MPa, gas flow 50–300 ml min^{-1})
2. the tube furnace (similar heating parameters)
3. the GC pyrolyzer (Pyroprobe 1000, 50 μg–5 mg sample, 30–1400 °C, dT/dt=10–20000 K s^{-1}, p=0.1–0.3 MPa, He flow 5–50 ml min^{-1})
4. the MS pyrolyzer (Pyroprobe 2000, 50 μg–5 mg sample, 30–800 °C, dT/dt=0.01–20000 K s^{-1}, $p \approx 1$ mPa).

The thermobalance is connected via a heated transfer line (stainless steel capillary, 250 °C) with the tube furnace. The quartz lined tube furnace is placed at the wall of the GC oven. During TG or furnace experiments the GC oven is kept at 250 °C.

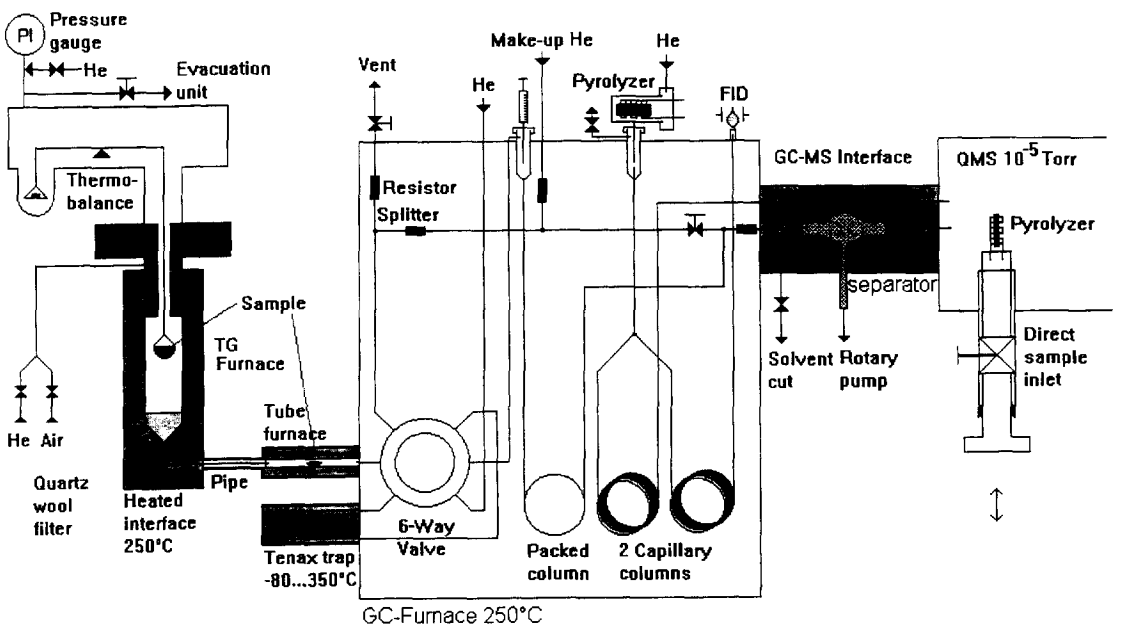

Fig. 1. Schematic presentation of the combined thermoanalytical apparatus.

Inside the GC oven a split system divides the gas flow such that a gas flow of only 5 ml min^{-1} enters the jet separator in front of the mass spectrometer. It is important to keep the split system at a constant temperature during any temperature-programmed pyrolysis run. The splitting of the gas flow directly above the sample, as is performed in several commercial coupling devices, effects a variable split ratio, which makes a quantitative analysis of the evolved products difficult.

The gas chromatograph is equipped with two capillary columns and one packed column (Tenax, 60–80 mesh). The available detectors include the QMS and an FID, which is suitable for quantification of pyrolysis-chromatograms. A Tenax-filled cold trap is installed between some of the pyrolysis reactors and the mass spectrometer in order to collect or to fractionate the pyrolysis products.

The first flash pyrolyzer (Pyroprobe 1000) is installed on one of the GC injectors (Py–GC–MS). It can quickly be changed between the capillary and the packed columns. The second flash pyrolyzer (Pyroprobe 2000) is introduced into the mass spectrometer through the direct sample inlet. The sample is positioned in front of the ion source (IS), such that the outlet of the sample tube matches the inlet opening of the ion source (ISPy–MS). The small quartz tubelets (18×2 mm) in the Pyroprobes are heated by a platinum coil, whereby the temperature of the coil, rather than that of the sample, is measured. Under high vacuum conditions, steep temperature gradients occur between the coil and the sample. Therefore, we installed an additional thermocouple (0.5 mm diameter) inside the quartz tube, in contact with the sample to be pyrolyzed. Even so, it is difficult to get a reliable measure of the actual sample temperature during the in-source pyrolysis. The temperature calibration by means of chemical thermometers is a well known method in chemical kinetics. We used the decomposition of several polymers in the thermobalance and in the in-source pyrolyzer, both with the same heating rate (10 K min^{-1}). This led to similar peak temperatures (T_{max}), e.g. for PTFE 588 and 604 °C, for PE 474 and 488 °C, for PS 418 and 449 °C, and for PVC 297 and 274 °C, respectively.

The calibration of MS signal intensities obtained with the various pyrolysis and coupling devices was performed by the injection of definite amounts of standard solutions into the GC, by thermal decomposition of polymers (Kraton, PE) or for light components (H_2O, CO, CO_2) by decomposition of salts ($CaOx \cdot H_2O$, $CaCO_3$).

For TG–FTIR coupling commercial equipment was available, consisting of a thermobalance TGA 7 and a FTIR spectrometer system 2000 (both from Perkin Elmer, Überlingen, Germany). The two units are connected by a heated transfer line (material: PEEK, 250 °C). The effluent from the thermobalance (50 ml min^{-1} He) was passed through the gas cell of the spectrometer, which was kept at 250 °C, with neither splitting nor dilution. The IR spectra were recorded with a resolution of 4 cm^{-1} in the range 4000 to 450 cm^{-1}.

3. Results

3.1. Identification of organic pollutants

Fig. 2 depicts a part of the total ion chromatogram (TIC) of a benzene extract of a typical wastewater, the analysis and remediation of which we are faced with.

Obviously, the dominant pollutants are phenols. The identification of this complex mixture was achieved using the mass spectral libraries and some well-known fragmentation rules. To improve assignments and to validate the cGC–MS results, the utilization of further hyphenated techniques is straightforward. The cGC–FTIR turned out to be not very helpful for this application, because it suffers from relatively small databases and low detection sensitivity, which often gave rise to overloaded, obscured and poorly resolved peaks in such extremely complex mixtures.

As can be seen from Fig. 2, there are many overloaded peaks in the TIC thus complicating the recognition of, e.g., heterocyclic compounds. However, the heterocyclic compounds are among the very pollutants which are of particular interest with regard to their sorption onto the HOM or their incorporation into the humic backbone. An ideal complement for their recognition is the cGC–AED coupling.

It is already evident from theoretical considerations that AED as an element-selective detection

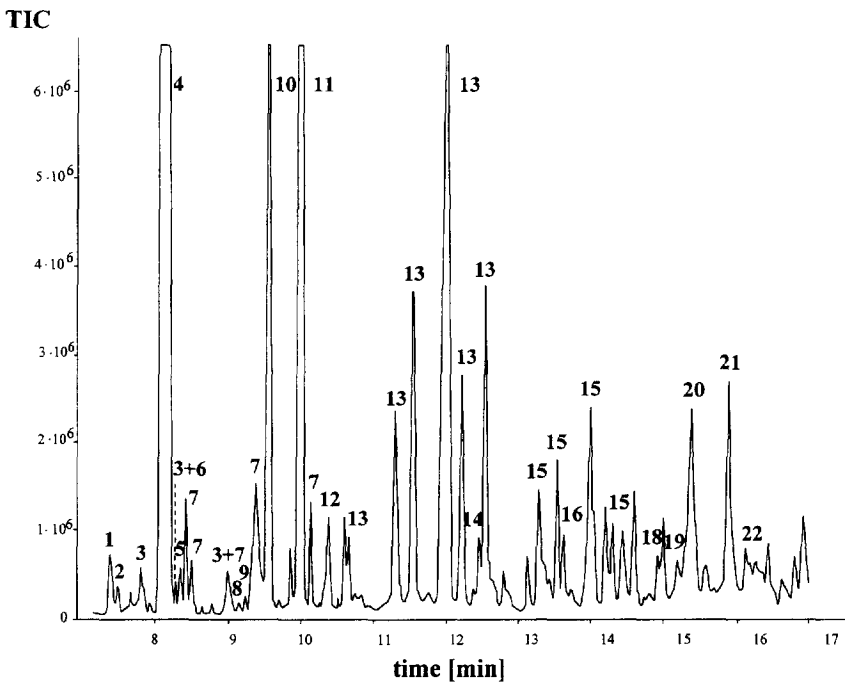

Fig. 2. Total ion chromatogram (TIC) of a benzene extract of the wastewater sampled from a depth of 25 m. Elemental composition and molecular ions are given in parentheses. 1 = 2-ethylcyclopentanone ($C_7H_{12}O/112$); 2 = cyclopentene-2-on-dimethyl ($C_7H_{10}O/110$); 3 = C_3-alkylbenzenes ($C_9H_{12}/120$); 4 = phenol ($C_6H_6O/94$); 5 = 1,3-cyclopentandione-4-ethyl ($C_7H_{10}O_2/126$); 6,6-methyl-2-heptanone ($C_8H_{16}O/128$); 7 = C_2-cyclopentene-1-one ($C_7H_{10}O/110$); 8 = 1,3-dimethyl-pyrazole ($C_5H_8N_2/96$) + unknown (124); 9 = unknown (118 + 124); 10 = *o*-cresol ($C_7H_8O/108$); 11 = *m*-, +*p*-cresol ($C_7H_8O/108$); 12 = C_3-cyclopentene-1-one ($C_8H_{12}O/124$) + unknown (96); 13 = C_2-phenols ($C_8H_{10}O/122$); 14 = naphthalene ($C_{10}H_8/128$); 15 = C_3-phenols ($C_9H_{12}O/136$); 16 = isoquinoline ($C_9H_7N/129$) + unknown (148); 17 = 1H-indene-1-one-2,3-dihydro ($C_9H_8O/132$); 18 = 2-methylnaphthalene ($C_{11}H_{10}/142$); 19 = 1-methyl-naphthalene ($C_{11}H_{10}/142$); 20 = 1H-indene-1-ol-2,3-dihydro ($C_9H_{11}O/134$); 21 = 1H-indene-5-ol-2,3-dihydro ($C_9H_{11}O/134$); 22 = methyl-1H-indene-1-ol-dihydro ($C_{10}H_{14}O/148$).

method is a better complement to the mainly structure-reflecting MS than the FTIR, as also a structure- or functionality-selective detector. Moreover, the main advantage of the FTIR technique, the recognition of isomers, is not so important for our purpose and may also be obtained-to some extent-by structure–retention relationships [9,10].

On the basis of estimated retention data we made a detailed mass spectrometric parameter retrieval, which succeeded in assigning the sulphur compounds as alkylated benzo[*b*]thiophenes. Unfortunately, the detection of sulphur compounds in higher retention intervals is hindered by an excessive peak of elemental sulphur (S_8). Analogously we succeeded in identifying specific nitrogen-containing constituents, including pyridine, pyrrole, indole, quinoline and their alkyl derivatives. However, we did not detect alkylated hydantoins, which were reported to be main the nitrogen-containing constituents of similar lignite wastewaters [11].

A combination of cGC–MS and cGC–AED was also utilized for qualification of the wastewater sediment extracts (chromatograms not shown). They were found to be even more complex than the water extracts. This can mainly be attributed to the pronounced alkane, 1-alkene, α,ω-alkadiene and alkylbenzene pattern characteristic of this sediment. After identifying the main target analytes in both wastewater and sediments they were quantified by using deuterated internal standards. If one assumes a partition-like sorption equilibrium of pollutants between the sediment organic matter and the waste-

water, one can calculate partition coefficients K_{OC} referred to the organic carbon content (OC) of the sediment:

$$K_{OC} = \frac{c_{sorbed}}{c_{dissolved}} \cdot \frac{100\%}{\%(w/w)\ OC}$$

The concentration of pollutants was determined in the bulk phase of the wastewater just above the sediment whereby it is assumed that the bulk phase is in equilibrium with the pore water. This seems to be justified because the wastewater pond is already in a stable state, at least in its deep region. Indeed, the sorption coefficients are in-situ values. Nevertheless, they follow the partition model, which is indicated by the close similarity between K_{OC} and K_{OW} values. These values, listed in Table 1, agree fairly well with literature data [12,13] for sorption of phenols and PAHs. They correlate with the octanol–water partition coefficients K_{OW}. This indicates the dominance of hydrophobic interactions in the sorption process, even for rather polar compounds such as phenol [15].

3.2. Matrix analysis with Py–GC methods

The characterization of particulate HOM from sediments and soils as well as of dissolved organic matter (DOM) isolated from aquifers has been a cumbersome and tedious matter (cf. [4,16,17] and literature cited therein). Such characterization can only be tackled by a combination of several analytical techniques, among which thermoanalytical methods may play an important role.

Conventional flash pyrolysis GC–MS is–under certain circumstances (see below)–a useful method for analyzing building blocks of polymeric organic matter [18–24], and enables us to distinguish between anthropogenic and natural HOM. In comparison to the natural humic matter, the pyrograms of the anthropogenic humic matter both of the wastewater and of the associated sediments show significantly higher quantities of phenols and benzenediols and a lower content of alkylfuranes (up to dibenzofuranes) and of methoxyphenols. Furanes are considered as markers of polysaccharide units, methoxyphenols as markers of lignin-derived units in the humic matter. As an example, Fig. 3 shows the pyrogram of a fulvic acid isolated from wastewater sampled from the pond at a depth of 26 m, just above the associated sediment.

cGC–AED coupling results reveal that the content of N- and S-containing heterocyclic compounds in the pyrograms is considerably higher for anthropogenic than for natural HOM. This corresponds with high contents of nitrogen and sulphur, e.g., 3.2 and 3.9% (w/w), respectively, in the anthropogenic fulvic acid. Model investigations with artificial HOM (generated by using hydroquinone and deuterated heterocyclic compounds) clearly prove an incorporation of the latter into the humic polymer backbone [25]. Therefore, we assume an incorporation of the heterocyclic pollutants from the lignite wastewater into the anthropogenic humic polymers. Fig. 4 shows the sulphur trace recorded by Py–cGC–AED of the wastewater fulvic acid. The AED is especially useful in the first part of the pyrogram, where many of overloaded and poorly resolved peaks occur, which cannot be recognized by cGC–MS alone.

Table 1
Concentration of some analytes in the wastewater and the associated sediment[a]

Organic pollutant	$c_{in\ water}$ (ppm)	$c_{in\ sediment}$ (ppm)	log K_{OC} [b]	log K_{OC} from [12], [13]	log K_{OW} from [14]
Phenol	164	315	0.91	1.18	1.49
Cresols	79	288	1.19	1.65	1.94
C_2-phenols	32	260	1.54	–	2.35
Naphthalene	0.21	49	3.00	3.1	3.35
Methylnaphthalenes	0.18	75	3.25	–	3.95
Fluorene	0.026	34	3.75	–	4.18
Phenanthrene	0.023	81	4.18	4.35	4.57
Pyrene	0.002	25	4.73	4.9	5.18

[a] The sediment was taken from the bottom of the wastewater pond (depth 26 m), the water from a depth of 25 m.
[b] Organic carbon content 23.5 wt%.

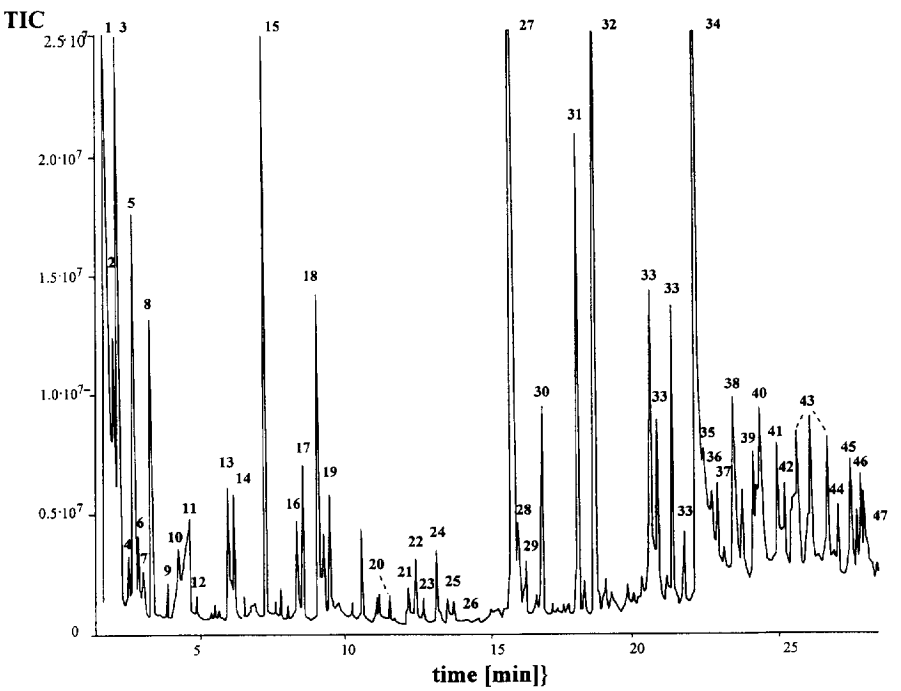

Fig. 3. Total ion pyrogram (10 s, 700 °C) of an anthropogenic fulvic acid isolated from the lignite wastewater (depth 25 m). Elemental composition and molecular ions are given in parentheses. 1 = hydrogen sulphide ($H_2S/34$) + carbon dioxide ($CO_2/44$); 2 = butenes ($C_4H_8/56$) + sulphur dioxide ($SO_2/64$); 3 = methanethiol ($CH_3SH/48$); 4 = isobutane ($C_4H_{10}/56$); 5 = acetonitrile ($CH_3CN/41$) + *n*-butane ($C_4H_{10}/58$); 6 = ethanethiol ($C_2H_5SH/62$); 7 = pentenes ($C_5H_{10}/70$) + propenenitrile ($C_3H_3N/53$); 8 = carbon disulphide ($CS_2/76$); 9 = propanenitrile ($C_3H_5N/55$); 10 = *n*-pentane ($C_5H_{12}/72$); 11 = acetic acid $CH_3COOH/60$); 12 = 2-methyl-propanenitrile ($C_4H_7N/69$); 13 = benzene ($C_6H_6/78$); 14 = thiophene ($C_4H_4S/84$); 15 = 3-hydroxy-2-pentene-1,5-lactone ($C_5H_8O_2/100$); 16 = pyridine ($C_5H_5N/79$); 17 = pyrrole ($C_4H_4N/67$); 18 = toluene ($C_7H_8/91$); 19 = methylthiophenes ($C_5H_6S/98$); 20, methylpyrroles ($C_5H_6N/81$); 21 = ethylbenzene ($C_8H_{10}/106$); 22 = *m*-/*p*-xylene ($C_8H_{10}/106$); 23 = dimethylthiophenes ($C_6H_8S/112$); 24 = styrene ($C_8H_8/104$); 25 = 2-cyclopentene-1-on-3-methyl ($C_6H_8O/96$); 26 = butyrolactone ($C_4H_6O_2/86$); 27 = phenol ($C_6H_5OH/94$); 28 = aniline ($C_6H_5NH_2/93$); 29 = benzonitrile ($C_6H_5CN/103$); 30 = imidazolidinethione ($C_3H_6N_2S/102$); 31 = *o*-cresol ($C_7H_8O/108$); 32 = *m*-/*p*-cresol ($C_7H_8O/108$); 33 = C_2-phenols ($C_8H_{10}O/122$); 34 = 1,2-benzenediol ($C_6H_6O_2/110$); 35 = C_3-alkylbenzenes ($C_9H_{12}/120$) + naphthalene ($C_{10}H_8/128$); 36 = benzo[*b*]thiophene ($C_8H_6S/134$); 37 = phenol-3-methoxy ($C_7H_8O_2/124$); 38 = C_3-phenols ($C_9H_{12}O/136$) + thieno-3,2-[*b*] thiophene ($C_6H_4S_2/140$); 39 = tetrahydrochinoline ($C_9H_{11}N/133$); 40 = 1,4-benzenediol ($C_6H_6O_2/110$); 41 = 5-hydroxy-2-furancarboxyaldehyde ($C_6H_6O_3/126$); 42 = 2,2′-bifuran ($C_8H_6O_2/134$); 43 = methylbenzenediols ($C_7H_8O_2/124$); 44 = dimethylbenzenediol ($C_8H_{10}O_2/138$) + 1,2-benzisothiazole-3(2H)-one ($C_7H_5NOS/151$); 45 = 3H-pyrazole-3-one,-2,4-dihydro-2,4,4,5-tetramethyl ($C_7H_{12}N_2O/140$) + C_4-phenol ($C_{10}H_{14}O/150$); 46 = methylbenzo[*b*]thiophene ($C_9H_8S/148$); 47 = dimethylbenzenediol ($C_8H_{10}O_2/138$).

On pyrolizing both river sediments and wastewater sediments we observed pronounced homologous series of *n*-alkanes and 1-alkenes with a proportion of approximately 1:2. This ratio is characteristic of a radical formation mechanism. It indicates that covalent C–C bonds in the aliphatic precursors had to be broken to release paraffins from the humic backbone.

The results obtained with Py–cGC–MS and Py–cGC–AED demonstrate the potential of these techniques to differentiate HOMs, e.g., natural from anthropogenic. However, results obtained with pyrolysis should be considered with caution to avoid misleading results and interpretations [26,27]. In our experience, the contribution of pyrolysis to the structural elucidation of HOM is sometimes overemphasized, insofar as the compounds released on pyrolyzing are considered to be representative of the polymeric network. In fact, only a small portion of the organic carbon is accessible for volatilization, even under high vacuum conditions. The protection of thermolabile groups by derivatization, e.g., by

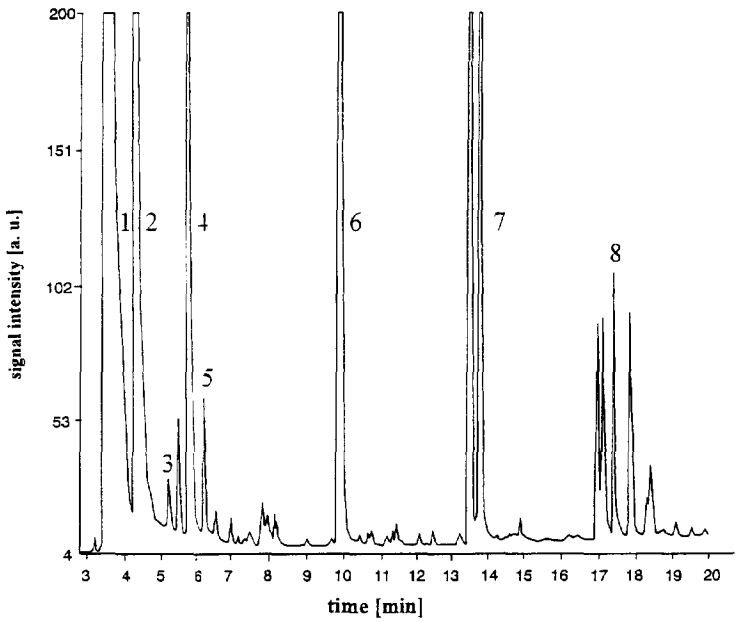

Fig. 4. Pyrogram from Py–GC–AED (10 s, 700 °C) for the sulphur emission line (180.7 nm) of an anthropogenic fulvic acid isolated from the wastewater. 1 = $COS + H_2S + SO_2$; 2 = CH_3SH; 3 = C_2H_5SH; 4 = CS_2; 5 = C_3H_7SH; 6 = thiophene; 7 = methylthiophenes; 8 = C_2-thiophenes.

pyrolysis-methylation with tetramethylammonium hydroxide (TMAH), is said to extend quantitatively and qualitatively the range of structural units accessible to Py–GC and Py–MS [28–33]. According to our results (see below) the extension appears to be only moderate. Nevertheless, pyrolysis-methylation is a useful tool for recognizing hydroxyl and carboxyl groups, which otherwise undergo dehydration and decarboxylation reactions on conventional pyrolysis. Some results obtained with both pyrolysis-methylation and conventional flash pyrolysis are presented in Figs. 5 and 6.

Prior to pyrolysis the wastewater sediment sample was thoroughly extracted with benzene–methanol (1:1) to remove sorbed hydrocarbons. The pyrolysis–methylation reveals a pronounced fatty acid methylester pattern. The tracing of the well-known McLafferty ion $m/z = 74$ (together with the ion $m/z = 87$) is strongly indicative of these methylesters. Palmitic acid methylester is dominant with about 60% of the total ester fraction. Paraffins ($m/z = 57$) are not significant pyrolysis products in the presence of TMAH at 500 °C. The apparently high concentration of fatty acids (as methyl esters) with a pronounced even over odd discrimination and the presence of unsaturated fatty acids give strong evidence for a significant biotic input to the wastewater sediment. This finding was surprising in view of the life-hostile conditions at the bottom of the wastewater pond.

By applying severe pyrolysis (800 °C) subsequently to the pyrolysis–methylation under moderate conditions (500 °C), a pyrogram is generated (Fig. 7) which is characterized by a homologous series of *n*-alkanes and 1-alkenes, while the fatty acids almost disappear. It is clear from both pyrograms that the precursors of the long-chain hydrocarbons are covalently bound onto the polymer backbone. They cannot be removed by solvent extraction or by thermodesorption (10 s, 350 °C). After scission of C–O ester bonds and evaporation of the released fatty acids (as methylesters) there remains an alkane pattern that we tentatively assign to long alkyl

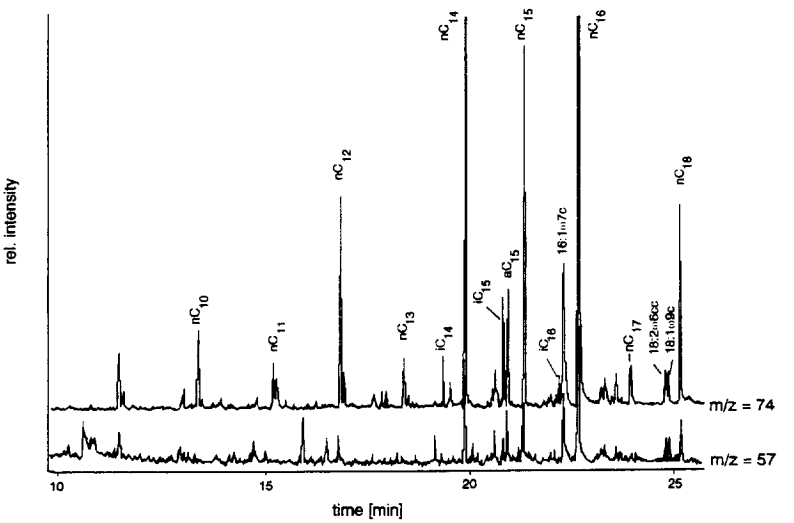

Fig. 5. Pyrogram from Py/Me–cGC–MS (10 s, 500 °C, TMAH) for selected ions of the wastewater sediment. The traces $m/z = 57$ and $m/z = 74$ represent long aliphatic chains and fatty acid methyl esters, respectively.

chains, which are connected to the polymer backbone via stable C–C bonds. These stable bonds are resistant against mild pyrolysis up to 500 °C and TMAH-induced chemolysis. A minor portion may result from an incomplete ester scission in the pyrolysis–methylation step. According to the Py– and Py/Me–cGC–MS results the fraction of C–C linked *n*-alkyl chains comes to about 20% of the

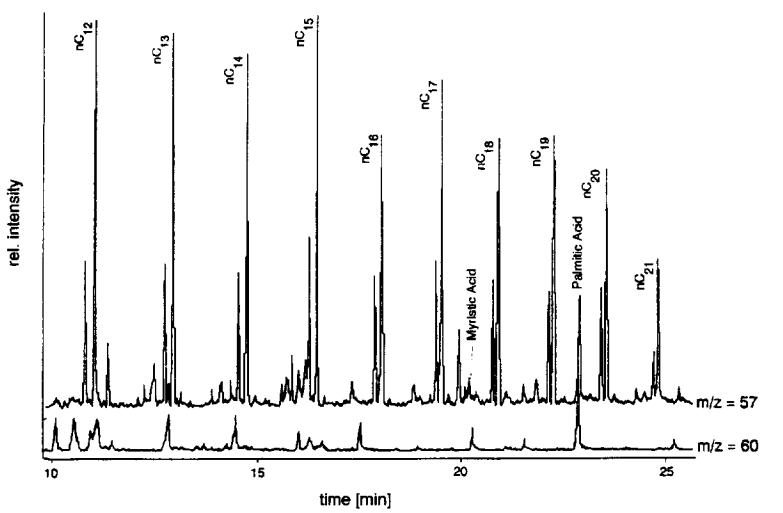

Fig. 6. Pyrogram from Py–cGC–MS (10 s, 800 °C) for selected ions of the wastewater sediment (after a preceding pyrolysis-methylation step at 500 °C, cf. Fig. 6). The traces $m/z = 57$ and $m/z = 60$ are indicative of fatty acids and *n*-alkanes, respectively.

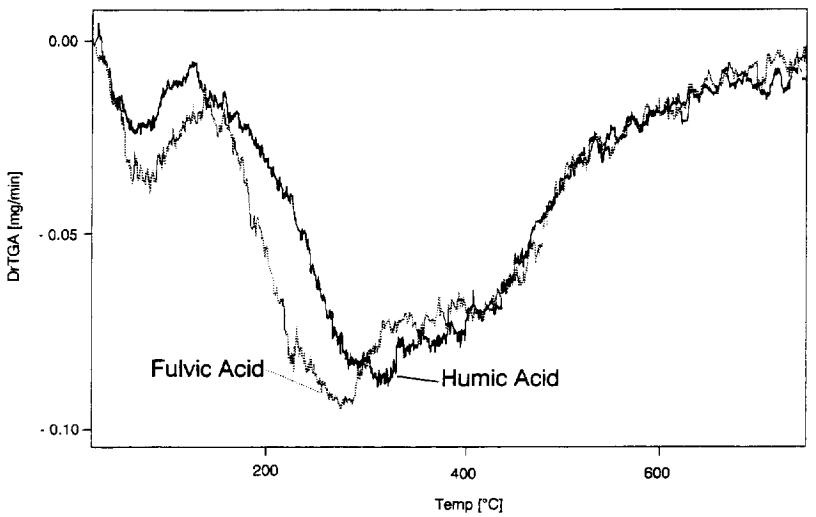

Fig. 7. DTG curves of the decomposition of ground-water fulvic and humic acid, experimental conditions: 5 mg sample, 30–750 °C, $dT/dt = 10$ K min^{-1}, 50 ml min^{-1} He flow.

total long alkyl chains in the anthropogenic polymer. The majority is loosely bound as fatty acid esters. In summary, the in-situ pyrolysis-methylation can give some further information on constituents of the HOM and their binding state.

3.3. Matrix analysis with other thermoanalytical techniques

A serious disadvantage of the Py–GC techniques is their low transfer efficiency for less volatile or highly polar pyrolysis products. Further thermoanalytical techniques may partly compensate for this and other shortcomings.

3.3.1. Thermogravimetry

The TG–MS coupling is known to be convenient for the routine analysis of synthetic polymers. For very complex samples, where the data evaluation takes much more time than the experiment, the time saving achievable with the coupling technique may be less important. On the other hand, the thermobalance may not be the optimal pyrolysis reactor due to the large gas flow to be handled and the large reactor volume, which favours secondary reactions. Therefore, we often decided to carry out separate pyrolysis runs with the same sample, each one under optimal conditions. The tube furnace used in our programmed heating experiments has an internal volume of about 0.5 ml, which is two orders of magnitude lower than that of the thermobalance reactor. Most of the following results are exemplified by two acids, both of them isolated from non-polluted ground water (alkaline regeneration of the ion-exchanger at the waterworks in Fuhrberg, Germany). Although not demonstrated in this study, the main conclusions are also valid for thermoanalysis of other humic substances. Fig. 7 shows two typical DTG curves, obtained for a fulvic acid (FA) and a humic acid (HA).

The first peak at 75 °C can be allocated to the evaporation of sorbed water. Generally, the DTG curves of humic substances are less specific. The decomposition of the organic matter starts already at about 120 °C, having one or two broad local maxima between 270 and 420 °C. The decomposition continues up to the final temperature of 750 °C, but the main mass loss is finished at about 600 °C. The FA has a higher content of thermolabile groups (weight loss below 300°C) compared with the HA. For both acids there remains a non-volatile residue of 36.6±0.6 wt% (w/w) (related to the dry organic matter), which was determined by burning off with air. This residue is highly carbonaceous in composition (>90%, w/w, C). Taking into account the carbon content of the acids (HA: 54.9%, w/w, FA:

52.0%, w/w), the pyrolysis residue comes to ≥66–70% of the original carbon. This portion has no diagnostic value for the humic polymer. In other words, two-thirds of the carbon pool are excluded from any structural evaluation. Even if the remaining third could be completely analyzed, it could not be considered to be representative of the whole polymer.

3.3.2. *In source pyrolysis–mass spectrometry*

The same two samples, FA and HA from ground water, were analyzed by ISPy–MS, which was run under high vacuum conditions instead of atmospheric pressure. Figs. 8 and 9 show the thermogram (TIC versus scan number, which is correlated with the sample temperature) and two averaged mass spectra, respectively, of the pyrolysis products of the fulvic acid.

The thermogram and mass spectra for the humic acid (not shown in this paper) are very similar to those for the fulvic acid. The sample was first treated in high vacuum at temperatures below 100 °C to desorb moisture, then it was placed in front of the inlet of the ion source. The first peak of the thermogram (100–180 °C) is due to a rapid heating of the sample by heat radiation from the ion source (250 °C). It is exclusively comprised of inorganic products (H_2O, CO_2, and SO_2). Most of the water and the carbon dioxide must be considered true decomposition products. The second peak (180–650 °C) includes many organic fragments. Fig. 9 shows that almost all the mass numbers are occupied. Above a mass range of about 110 u the mass spectrum does not contain relevant information on the sample. This is due to the very complex pattern of the pyrolysis products and their extensive fragmentation by 70 eV EI. It is apparent that a few low molecular weight substances dominate the spectrum of the pyrolysis products. These are methane (m/z = 15 and 16), water (m/z = 17 and 18), carbon monoxide (m/z = 28), carbon dioxide (m/z = 44) and sulphur dioxide (m/z = 64). Some signals can be tentatively attributed to groups of organic compounds, such as m/z = 60 for carbonic acids, m/z = 77 for phenyl groups, m/z = 91 and 105 for alkylbenzenes, m/z = 94 and 107 for phenols etc. Fig. 10 shows some characteristic thermograms of selected marker ions.

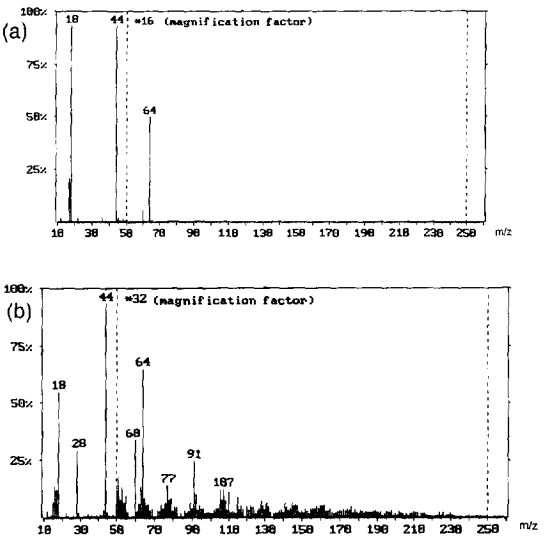

Fig. 9. Averaged pyrolysis mass spectra of a ground-water fulvic acid obtained by ISPy–MS, 1st peak: 100–180 °C (a), 2nd peak: 180–600 °C (b), experimental conditions as described in Fig. 8.

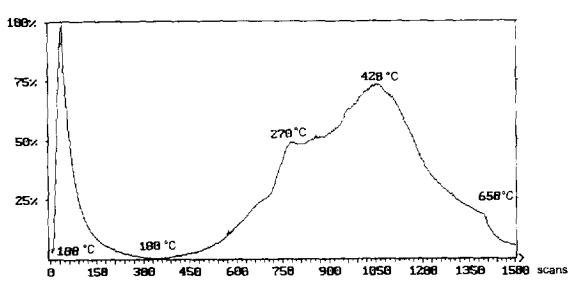

Fig. 8. Thermogram (TIC) of a ground-water fulvic acid, obtained by ISPy–MS, experimental conditions: 500 μg sample, 100–650 °C, $dT/dt \approx 10$ K min^{-1}, p = 1 mPa, 70 eV EI, scan width 10–500 u, scan rate 0.33 Hz.

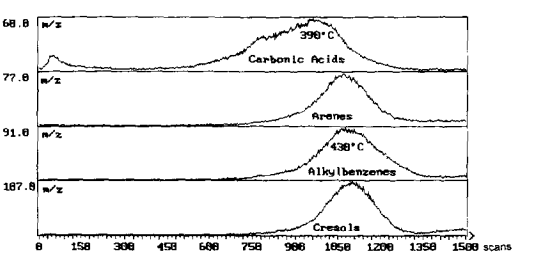

Fig. 10. Thermograms of selected ions from the ISPy–MS of a ground-water fulvic acid, experimental conditions as described in Fig. 9.

They indicate a well defined range where the organic matrix is broken down. Paraffinic fragments (m/z=55, 57, 69, 71) were not observed in the pyrolysis mass spectra. This is a remarkable distinction between the two ground-water humic substances and soil humic acids, which usually have a prominent paraffinic fraction. The peak maxima of the aromatic fragments are around 400 °C. This temperature corresponds with the second maximum in the DTG curve. The first DTG maximum at about 280 °C coincides with the maximum in the CO_2 evolution curve. Briefly spoken, the two steps in the humic substance degradation are the splitting-off of functional groups and the breakdown of the polymer network.

The carbonaceous residues of the vacuum pyrolysis were also gravimetrically measured: 41 and 45 wt% for the fulvic and the humic acid, respectively. These values are close to the coke yields obtained under atmospheric pressure, with the same final pyrolysis temperature (at 650 °C 40 and 41 wt%). Thus, the high vacuum pyrolysis does not favour the evolution of organic components over the splitting-off of functional groups. This can be explained by the assumption that the relative rates of chemical reactions control the product pattern, not a transport limitation.

The heating rate is another important parameter which determines the product pattern of pyrolysis reactions [18]. The flash pyrolysis of the ground-water fulvic acid under conditions typical of Py–GC experiments (0.5 mg sample, T_{set}=800 °C, 10 s, $dT/dt \geq 10^2$ K s^{-1}, p=0.2 MPa) yielded about 40% (w/w) of residue. Results similar to these presented in this paper for two aquatic humic substances were also obtained with other humic substances, including soil humic acids and non-extracted humic matter (whole soils and sediments). Apparently, the undesired reaction channel leading to the formation of non-volatile, carbonaceous residues cannot be efficiently suppressed for humic substances. A flash pyrolysis under vacuum conditions, which could be a useful alternative, can hardly be realized with grained samples, because the heat transition from any heating element (e.g., a Curie-point wire) to the sample is rather slow.

The volatile products from ISPy–MS were quantified in two different ways:

1. From the average pyrolysis mass spectrum we calculated the portion of inorganic (m/z=17, 18, 28, 44, 64) and organic signal intensities (all ions with m/z=10–500, except the preceding ones) and
2. we calculated yields (related to the weight loss of the dry sample) of some pyrolysis products, for which calibration factors were available.

The results are as follows: 73% (FA) and 65% (HA) of the total signal intensity come from the inorganic products (H_2O, CO, CO_2), only 27% to 35% from organic products. From fulvic acid the yields of water, carbon monoxide, carbon dioxide and methane are 20, 17, 30 and 2.5% (w/w) of the volatiles (Σ 69.5%), respectively. From humic acid they are 18, 15, 27 and 1.5% (w/w) (Σ 61.5%). These data illustrate that even the volatile fraction consists mainly of non-specific pyrolysis products. This is the second source of information loss on the original structure beside the coke residue. A mass balance of pyrolysis products leads to 18% (w/w) [=(1−0.695)·(1−0.41)] and 21% (w/w) [=(1−0.615)·(1−0.45)] of organic pyrolysis products from the fulvic and the humic acid, respectively. The yields correspond well with those calculated from the sum of the signals of all organic fragments, if an averaged calibration factor from pyrolysis of synthetic polymers is used (15 and 21 wt% of organic compounds from FA and HA, respectively).

It is interesting to compare the yields of pyrolysis products with the elemental composition and the concentration of functional groups in the humic substances. The concentration of carboxylic and phenolic groups was determined by titration of the acidity in the two pH ranges 3.0–7.5 and 7.5–10.5 [34]. For the ground-water fulvic and humic acids the following data were determined: $c_{\text{-COOH}}$=5.05 mval g^{-1} and $c_{\text{Ar-OH}}$=1.00 mval g^{-1}; elemental analysis (related to the dry organic matter): 52.2% (w/w) C, 3.97% (w/w) H, 1.21% (w/w) N, 1.08% (w/w) S, about 40% (w/w) O (from balance). A content of 5.05 mval g^{-1} -COOH corresponds with 22.2% (w/w) of CO_2. The yield of CO_2 in the pyrolysis products from the FA was found to be 17.7% (w/w) [=30·(1−0.41)]. Formally considered this means about 80% of the carboxylic groups decarboxylate. The sum of oxygen pushed out as

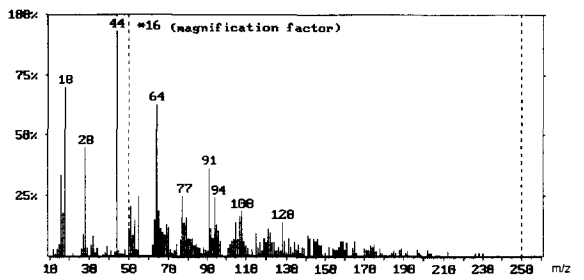

Fig. 11. Averaged mass spectrum of a ground-water fulvic acid obtained by ISPy methylation–MS in the temperature range 180–650°C, experimental conditions as described in Fig. 9 (1 mg sample).

water and carbon oxides comes to 29% (w/w) [(1 − 0.41)·(20·16/18 + 17·16/28 + 30·32/44)]. This is about 72% of the total oxygen in the FA. These calculations clearly demonstrate that the majority of oxygen containing groups are lost in the course of the conventional pyrolysis. Unfortunately, very few papers on analytical pyrolysis of humic and related substances examine critically the quantification aspect. Where this has been done [18,33,35,36], the conclusions are as cautious as in the present paper.

The alternative of pyrolysis-methylation under high vacuum does not change the picture decisively. Fig. 11 shows the averaged mass spectrum of the pyrolysis products in the temperature range 180–650 °C, after the decomposition of TMAH is finished.

The mass spectrum is similar to that obtained without derivatization, except that the intensity of the signals of organic fragments is increased (magnification factor 16 instead of 32 in Fig. 9) and no signal of carbonic acids ($m/z = 60$) is detected. It is evident that the inorganic products water and carbon oxides dominate again. Some minor changes in the mass spectrum may not be significant, because it is corrected by the background from the TMAH decomposition and some signal intensities are close to the background. The expected derivatization products, carbonic acid methyl esters ($m/z = 74$), are missing in Fig. 11. This is because the formed methyl esters desorb rapidly in high vacuum, such that they appear in the low temperature peak (< 180 °C, not depicted). The pyrolysis residue amounts to ≥32% (w/w) related to the dry fulvic acid. This is less than the residue from the untreated fulvic acid (41 wt%), but still a large portion of it is organic carbon (62%). A quantification of the ISPy methylation–MS results is difficult, because of the presence of an abundance of TMAH and its decomposition products. Semiquantitatively, it can be estimated that the splitting-off of functional groups from humic substances can be moderately decreased, but not significantly suppressed by the procedure applied in this study.

3.3.3. *Thermogravimetry–FTIR spectroscopy*

Sometimes it can be difficult to detect unambiguously low-molecular-mass compounds such as carbon dioxide, carbon monoxide, water, methane, sulphur dioxide, COS and ammonia by mass spectrometry only, because their marker ions can be masked by intensive signals of other fragment ions. In this context the TG–FTIR coupling may be a valuable complementary technique. A well-defined absorption band can be assigned to each of the above compounds. Table 2 lists the products detected.

Further complementary information to that from the TG–MS technique comes from the fact that wavenumbers in infrared spectra can be – to some extent – directly assigned to a structural unit. For example the bands around 3000 cm^{-1} can be as-

Table 2
Low molecular mass compounds released on heating the wastewater sediment, detected by TG–FTIR

Compound	Characteristic wavenumber (cm^{-1})	Temperature range of appearance (°C)	Temperature with maximum absorbance (°C)
CH_4	3012	380–535	470
CO_2	2335	50–750	335, 665
CO	2190	410–750	695
COS	2070	280–460	365
H_2O	1515	50–110, 235–400	80, 305
SO_2	1370	210–535	285
NH_3	960	190–670	325, 550

signed to hydrocarbon units, whereas the recognition of all the hydrocarbon units by means of the MS technique is a rather strenuous task. Considering the fact that both thermogravimetry and FTIR are accomplished at atmospheric pressure rather than under high vacuum conditions, the TG–FTIR coupling can also be utilized for quantification purposes.

4. Conclusions

The analysis of organic pollutants in a wastewater rich in polymeric organic matter can be performed by conventional methods, such as solvent extraction followed by cGC–MS and cGC–AED analysis of the extracts. A further source of pollutants is the associated sediment at the bottom of the wastewater pond. These sediment pollutants were analyzed using the same hyphenated techniques after supercritical fluid extraction rather than solvent extraction. The most difficult problem is the characterization of the dissolved and particulate organic polymers, which have been formed in the wastewater pond for some decades. They have properties similar to natural humic matter. Therefore we call them anthropogenic humic matter.

The application of several thermoanalytical techniques, such as Py–cGC–MS, in source Py–MS and TG–FTIR, on ground-water humic substances allowed some insight into their composition. However, quantitative considerations give evidence that pyrolysis is able to visualize only a small cutout of the original polymer structure. The main products are a carbonaceous residue, formed by splitting off of functional groups accompanied by cross-linking reactions, and low molecular mass products with little diagnostic value, such as water and carbon oxides. These undesired reactions seem to be hardly avoidable, even under high vacuum conditions.

Acknowledgments

This work was partly supported by the Deutsche Forschungsgemeinschaft and the Deutsche Bundesstiftung Umwelt. The authors thank Mrs. B. Dommsch and Mrs. C. Anton for their excellent technical assistance.

References

[1] A. Wiessner, P. Kuschk, E. Weissbrodt, U. Stottmeister, J. Pörschmann and F.-D. Kopinke, Wasser-Abwasser-Praxis, 1993 (6), 375.
[2] J. Pörschmann and U. Stottmeister, Chromatographia, 36 (1993) 207.
[3] F.H. Frimmel and R.F. Christman (Editors), Humic Substances and their Role in the Environment, Wiley, Chichester, 1988.
[4] B.H.M. Hayes, P. MacCarthy, R.L. Malcolm and R.S. Swift (Editors), Humic Substances II. In Search of Structure, Wiley, Chichester, 1989.
[5] I.H. Suffet and P. Mac Carthy (Editors), Aquatic Humic Substances. Influence on Fate and Treatment of Pollutants, Advances in Chemistry Series 219, American Chemical Society, Washington, 1989.
[6] J. Pörschmann et al., in preparation.
[7] Sh. Kuwatsuka, A. Watanabe, K. Itoh and Sh. Arai, Soil Sci. Plant Nutr., 38 (1992) 23.
[8] K. Wienhold and G. Hanschmann, Chem. Techn., 43 (1991) 232.
[9] W. Engewald, J. Pörschmann and T. Welsch, Chromatographia, 30 (1990) 537.
[10] C.T. Peng, J. Chromatogr. A, 678 (1994) 189.
[11] M.F. Giabbai, W.H. Cross, E.S.K. Chian and F.B. Dewalle, Int. J. Environ. Anal. Chem., 20 (1985) 113.
[12] S.W. Karickhoff, D.S. Brown and T.A. Scott, Water Res., 13 (1979) 241.
[13] J.C. Means, S.G. Wood, J.J. Hassett and W.L. Banwart, Environ. Sci. Technol., 14 (1980) 1524.
[14] M.J. Kamlet, R.M. Doherty, M.A. Abraham, Y. Marcus and R.W. Taft, J. Phys. Chem., 92 (1988) 5244.
[15] F.-D. Kopinke, J. Pörschmann and U. Stottmeister, Environ. Sci. Technol., 29 (1995) 941.
[16] R.E. Engebretson and R.V. Wandruszka, Environ. Sci. Technol., 28 (1994) 1934.
[17] H.-R. Schulten and M. Schnitzer, Naturwissenschaften, 82 (1995) 487.
[18] J.M. Bracewell, K. Haider, S.R. Larter and H.-R. Schulten, in ref. [3], chapter 7, pp. 182, Thermal Degradation Relevant to Structural Studies of Humic Substances, 1988.
[19] C. Saiz-Jimenez, Sci. Total Environ., 117/118 (1992) 13.
[20] C. Saiz-Jimenez, J.J. Ortega-Calvo and B. Hermosin, Naturwissenschaften, 81 (1994) 28.
[21] N. Simmleit and H.-R. Schulten, J. Anal. Appl. Pyrol., 15 (1989) 3.
[22] H.-R. Schulten, J. Anal. Appl. Pyrol., 25 (1993) 97.
[23] H.-R. Schulten and M. Schnitzer, Soil Sci., 153 (1992) 205.
[24] H.-R. Schulten and P. Leinweber, Plant and Soil, 151 (1993) 77.
[25] J. Pörschmann et al., in preparation.
[26] C. Saiz-Jimenez, Environ. Sci. Technol., 28 (1994) 1773.
[27] C. Saiz-Jimenez, J.J. Ortega and B. Hermosin, Naturwissenschaften, 81 (1994) 28.
[28] J.W. de Leeuw and M. Baas, J. Anal. Appl. Pyrol., 26 (1993) 175.

[29] J.M. Challinor, J. Anal. Appl. Pyrol., 25 (1993) 349 and 35 (1995) 93.
[30] D.E. McKinney, D.M. Carson, D.J. Clifford, R.D. Minard and P.G. Hatcher, J. Anal. Appl. Pyrol., 34 (1995) 41.
[31] P. Leinweber and H.-R. Schulten, Mitteil. Dtsch. Bodenkundl. Gesell., 76 (1995) 1389.
[32] F. Martin, F.J. Gonzales-Vila, J.C. del Rio and T. Verdejo, J. Anal. Appl. Pyrol., 28 (1994) 71; 31 (1995) 75; 35 (1995) 1.
[33] G. Chiavari, G. Torsi, D. Fabbri and G.C. Galletti, Analyst, 119 (1994) 1141.
[34] F.H. Frimmel, W. Hopp and K.E. Quentin, Wasser-Abwasser-Forsch., 18 (1985) 259.
[35] W.M.G.M. van Loon and J.J. Boon, Trends Anal. Chem., 13 (1994) 169.
[36] J.M. Bracewell and G.W. Robertson, J. Anal. Appl. Pyrol., 6 (1984) 19.